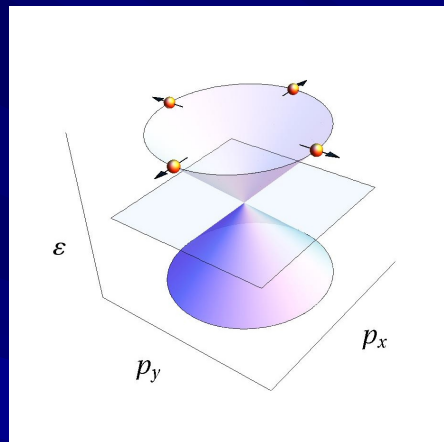


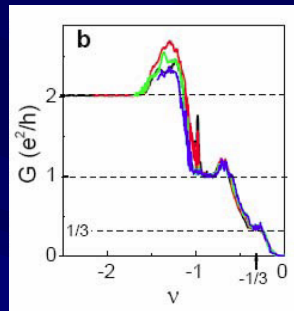
QUANTUM ELECTRODYNAMICS OF 2D AND 3D DIRAC SEMIMETALS



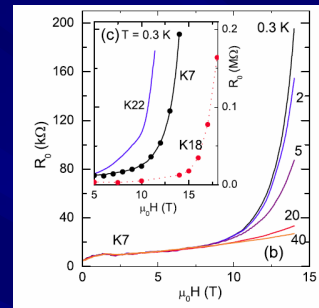
J. González
Instituto de Estructura de la Materia, CSIC, Spain

2D DIRAC SEMIMETALS

Interaction effects have been observed in graphene, in particular under the influence of a magnetic field:

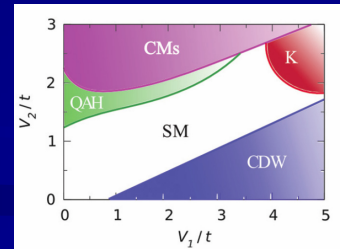
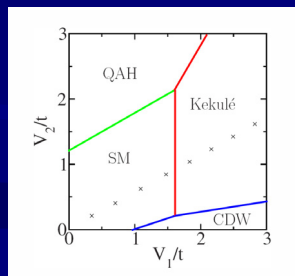


X. Du *et al.*, Nature **462**, 192 (2009).



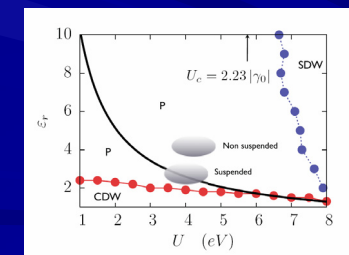
J. G. Checkelsky *et al.*, PRL **100**, 206801 (2008).

Moreover, theoretical studies have shown that correlated phases may arise in the honeycomb lattice under sufficiently large Coulomb repulsion



C. Weeks and M. Franz, Phys. Rev. B **81**, 085105 (2010)

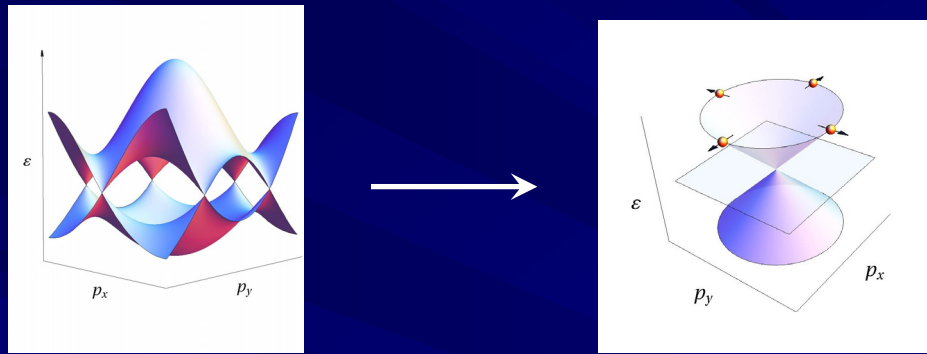
A. G. Grushin *et al.*, Phys. Rev B **87**, 085136 (2013)



J. Jung and A. H. MacDonald, Phys. Rev. B **84**, 085446 (2011)

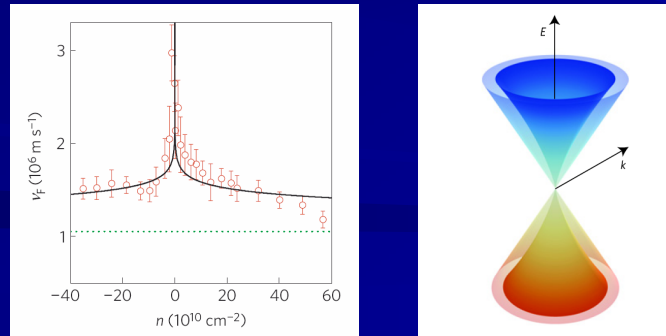
2D DIRAC SEMIMETALS

2D Dirac semimetals like graphene are naturally placed in the strong-coupling regime:



Is the gapless conical dispersion preserved down to the Dirac point in the interacting electron system?

Experiments carried out in graphene at very low doping levels seem to imply an affirmative answer:



D. C. Elias *et al.*, Nature Phys. 7, 701 (2011)

2D DIRAC SEMIMETALS

There have been many analyses of the dynamical generation of a gap in graphene:

- **Gap equation, 1/N approximation**, D. V. Khveshchenko, PRL 87, 246802 (2001);
E. V. Gorbar, V. P. Gusynin, V. A. Miransky and I. A. Shovkovy, PRB 66, 045108 (2002).
- **Gross-Neveu interactions**, I. F. Herbut, V. Juricic and O. Vafek, PRB 80, 075432 (2009);
V. Juricic, I. F. Herbut and G. W. Semenoff, PRB 80, 081405 (2009).
- **Lattice field theory**, J. E. Drut and T. A. Lähde, PRL 102, 026802 (2009); PRB 79, 241405(R)
(2009) \Rightarrow critical $\alpha_c \approx 1.08$
(see also W. Armour, S. Hands, C. Strouthos, PRB 81, 125105 (2010))
- **Ladder approximation**, J. Wang, H. A. Fertig and G. Murthy, PRL 104, 186401 (2010);
gap equation, static polarization, O. V. Gamayun, E. V. Gorbar and V. P. Gusynin, PRB 80,
165429 (2009) \Rightarrow critical $\alpha_c \approx 1.62$
- **Gap equation, dynamical screening**, O. V. Gamayun, E. V. Gorbar and V. P. Gusynin, PRB
81, 075429 (2010) \Rightarrow critical $\alpha_c \approx 0.92$
- **Effect of Fermi velocity renormalization**, J. Sabio, F. Sols and F. Guinea, PRB 82, 121413(R)
(2010); J. G., PRB 85, 085420 (2012) \Rightarrow critical $\alpha_c \gtrsim 3.8$
- **Lattice field theory revisited**, M. V. Ulybyshev, P. V. Buividovich, M. I. Katsnelson, and M.
I. Polikarpov, PRL 111, 056801 (2013) \Rightarrow critical $\alpha_c > 2.2$

2D DIRAC SEMIMETALS

We will focus on the effects of the long-range Coulomb interaction

$$S = \int dt d^2x \Psi_\sigma^+(\mathbf{x}) (i\partial_t - i\nu_F \gamma_0 \boldsymbol{\gamma} \cdot \boldsymbol{\partial}) \Psi_\sigma(\mathbf{x}) - \frac{e^2}{8\pi} \int dt d^2x d^2x' \Psi_\sigma^+(\mathbf{x}) \Psi_\sigma(\mathbf{x}) \frac{1}{|\mathbf{x} - \mathbf{x}'|} \Psi_{\sigma'}^+(\mathbf{x}') \Psi_{\sigma'}(\mathbf{x}')$$

In systems like graphene, we face then the strong-coupling regime, with a nominal interaction strength

$$\alpha = \frac{e^2}{4\pi\nu_F} \approx 2.2 \quad (\text{suspended graphene samples})$$

In these conditions, the electron system should be prone to develop condensation with

$$\langle \Psi^+(\mathbf{r}) M \Psi(\mathbf{r}) \rangle \neq 0$$

$$\int dt d^2x \Psi_\sigma^+(\mathbf{x}) (i\partial_t - i\nu_F \gamma_0 \boldsymbol{\gamma} \cdot \boldsymbol{\partial}) \Psi_\sigma(\mathbf{x}) \rightarrow \int dt d^2x \Psi_\sigma^+(\mathbf{x}) (i\partial_t - i\nu_F \gamma_0 \boldsymbol{\gamma} \cdot \boldsymbol{\partial} - m M) \Psi_\sigma(\mathbf{x})$$

In the representation $(\psi_{AK} \ \psi_{BK} \ \psi_{AK'} \ \psi_{BK'})$, the order parameters for the opening of a gap correspond to

$$M = \sigma_3 \otimes \mathbf{1} , \ \sigma_3 \otimes \tau_3 , \ \sigma_1 \otimes \tau_1 , \ \sigma_1 \otimes \tau_2$$

2D DIRAC SEMIMETALS

Arranging the spinors in the two valleys of graphene as $(\psi_{AK} \ \ \psi_{BK} \ \ \psi_{AK'} \ \ \psi_{BK'})$, we can have:

- parity-invariant mass term (G. W. Semenoff, PRL 53, 2449 (1984)):

$$H = m_0 \int d^2r \ \Psi^+(\mathbf{r}) \begin{pmatrix} \sigma_3 & 0 \\ 0 & \sigma_3 \end{pmatrix} \Psi(\mathbf{r})$$

breaks chiral symmetry $CS : \Psi(\mathbf{r}) \rightarrow (\sigma_2 \otimes \tau_2) \Psi(\mathbf{r})$

- Haldane mass term (F. D. M. Haldane, PRL 61, 2015 (1988)):

$$H = m_H \int d^2r \ \Psi^+(\mathbf{r}) \begin{pmatrix} \sigma_3 & 0 \\ 0 & -\sigma_3 \end{pmatrix} \Psi(\mathbf{r})$$

breaks invariance under parity $P_x : \Psi(x, y) \rightarrow (\mathbf{1} \otimes \tau_1) \Psi(-x, y)$

and it also breaks time-reversal symmetry $T = KP$, with

$$P : \Psi \rightarrow (\mathbf{1} \otimes \tau_1) \Psi$$

2D DIRAC SEMIMETALS

Quasiparticle properties can be studied in a large- N approximation

$$\Sigma(\mathbf{k}, \omega) = \sum_{n=1}^{\infty} \text{Diagram } n$$

$$\begin{aligned} \frac{1}{G} &= \frac{1}{G_0} - \Sigma \\ &\approx \omega - v_F \boldsymbol{\sigma} \cdot \mathbf{k} \\ &\quad + (A(\alpha) \omega - B(\alpha) v_F \boldsymbol{\sigma} \cdot \mathbf{k}) \log(\Lambda / \omega) \end{aligned}$$

$$\alpha \equiv \frac{e^2}{4\pi v_F}$$

The quasiparticle weight and the Fermi velocity are renormalized at low energies

$$G(\mathbf{k}, \omega) = \frac{Z_\psi}{\omega - v_F Z_\psi \boldsymbol{\sigma} \cdot \mathbf{k} + i\Gamma(\omega)}$$

$$Z_\psi(\omega) \approx 1 - a \alpha^2 \log(\Lambda / \omega) \quad a > 0$$

$$Z_v(\omega) \approx 1 + a' \alpha \log(\Lambda / \omega) \quad a' > 0$$

$$\Gamma(\omega) \sim \alpha^2 \omega$$

The reduction of the effective coupling $\alpha \equiv e^2/4\pi v_F$ governs the behavior of the system and is responsible of rendering the quasiparticle weight finite at low energies

$$\alpha \sim \frac{1}{\log\left(\frac{\Lambda}{\omega}\right)} \quad , \quad \text{Im } \Sigma \sim \frac{\omega}{\log^2\left(\frac{\Lambda}{\omega}\right)} \Leftrightarrow \text{Re } \Sigma \sim \frac{\omega}{\log\left(\frac{\Lambda}{\omega}\right)}$$

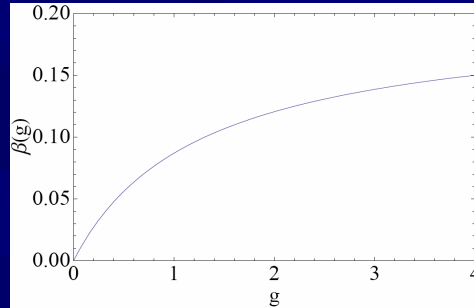
(J. G., F. Guinea and
M. A. H. Vozmediano,
Phys. Rev. Lett. **77**, 3589 (1996))

2D DIRAC SEMIMETALS

The advantage of the large- N approximation is that it allows to study the behavior of the system for arbitrarily large coupling. In terms of $g = Ne^2/32 v_F$

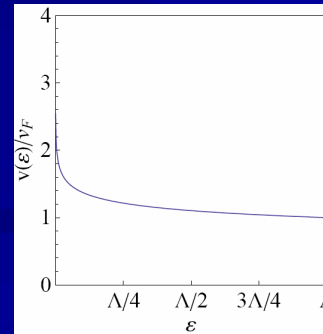
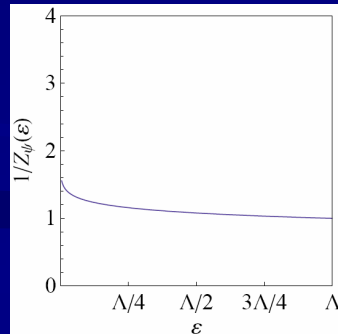
$$\varepsilon \frac{\partial}{\partial \varepsilon} \log Z_\psi(\varepsilon) = \frac{1}{N} \gamma(g)$$

$$\varepsilon \frac{\partial}{\partial \varepsilon} v_F(\varepsilon) = -\frac{1}{N} \beta(g)$$



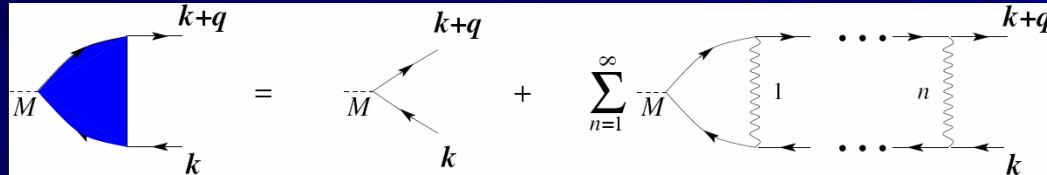
(J. G., F. Guinea and
M. A. H. Vozmediano,
Phys. Rev. B 59, R2474 (1999))

The behavior of the Fermi velocity is in agreement with the experimental observations at very low doping levels



2D DIRAC SEMIMETALS

However, the large- N approximation is not the right approach to look for some effects, like the condensation of electron-hole pairs. We have to shift to a complementary approach



Then we can study the condensation of a given fermion density $\rho_M(\mathbf{r}) = \Psi^+(\mathbf{r}) M \Psi(\mathbf{r})$ by looking for critical points where the vertex

$$\Gamma_M(\mathbf{q}, \omega_q; \mathbf{k}, \omega_k) = \langle \rho_M(\mathbf{q}, \omega_q) \Psi(\mathbf{k} + \mathbf{q}, \omega_k + \omega_q) \Psi^+(\mathbf{k}, \omega_k) \rangle \quad \text{blows up.}$$

In the above ladder approximation (static RPA screening), the equation for the vertex becomes

$$\Gamma_M(0; \mathbf{k}) = M + \pi \lambda_0 \int \frac{d^{2-\varepsilon} p}{(2\pi)^2} \Gamma_M(0; \mathbf{p}) \frac{1}{|\mathbf{p}|} \frac{1}{|\mathbf{p} - \mathbf{k}|} \quad \lambda_0 = \frac{\mu^\varepsilon e^2}{4\pi\kappa v_F}$$

In the resolution, we still have to get rid of divergences in the high-energy cutoff ε , which leads to the scale dependence of the renormalized vertex

$$\Gamma_M(0; \mathbf{k}) \Big|_{\text{ren}} = Z_M \Gamma_M(0; \mathbf{k}) \quad \Rightarrow \quad \Gamma_M(0, \mathbf{k}) \Big|_{\text{ren}} \sim \left(\frac{\mu}{|\mathbf{k}|} \right)^\gamma, \quad \gamma_M = \frac{\mu}{Z_M} \frac{\partial Z_M}{\partial \mu}$$

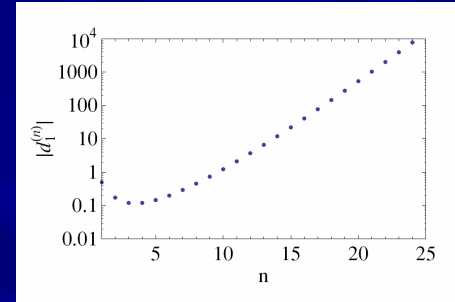
2D DIRAC SEMIMETALS

The anomalous exponent is

$$\gamma_M = \frac{\mu}{Z_M} \frac{\partial Z_M}{\partial \mu} = -\lambda d'_1(\lambda) \quad , \quad Z_M = \sum_{n=1}^{\infty} \frac{d_j(\lambda)}{\epsilon^n} \quad \lambda = \frac{e^2}{4\pi\kappa v_F}$$

γ_M has an expansion in λ , which can be computed up to very large orders from

$$d_1(\lambda) = \sum_{n=1}^{\infty} d_1^{(n)} \lambda^n$$



For the usual CDW order parameter $\rho_M(\mathbf{r}) = \Psi^+(\mathbf{r}) \gamma_0 \Psi(\mathbf{r})$, the power series has a finite radius of convergence

$$\lambda_c \approx 0.456947$$

(J. G., JHEP 08, 27 (2012))

which coincides precisely with the critical coupling obtained from the gap equation

$$\lambda_c = 8\pi^2/(\Gamma(1/4))^4$$

(O. V. Gamayun *et al.*, PRB 80, 165429 (2009))

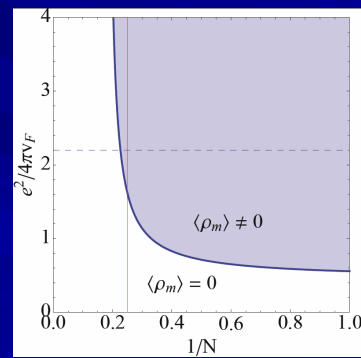
2D DIRAC SEMIMETALS

Anyhow, we have to bear in mind that λ is the coupling for the screened interaction,

$$\lambda = \frac{e^2}{4\pi\kappa v_F}$$

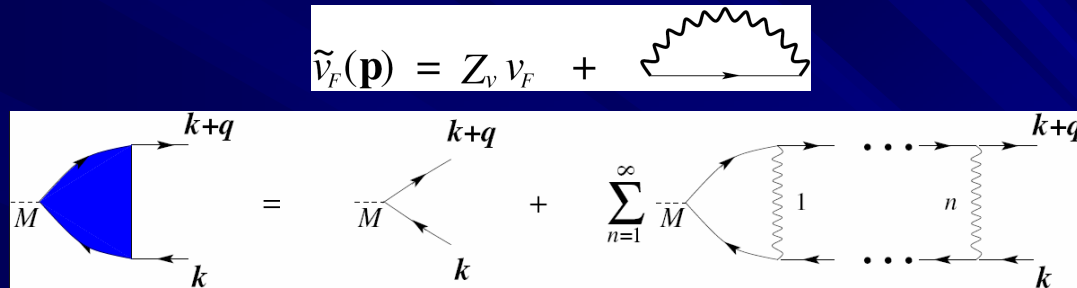
Its relation to the nominal coupling $\alpha = e^2/4\pi v_F$ depends on the screening effects and, under a static RPA,

$$\lambda = \frac{\alpha}{1 + \frac{N\pi}{8}\alpha} \quad \Rightarrow \quad \alpha_c = \frac{\lambda_c}{1 - \frac{N\pi}{8}\lambda_c}$$



2D DIRAC SEMIMETALS

The above approach can be improved by including the effect of electron self-energy corrections



$$\Gamma_M(0; \mathbf{k}) = M + ie_0^2 \int \frac{d\omega_p}{2\pi} \frac{d^{2-\varepsilon} p}{(2\pi)^2} G(\mathbf{p}, \omega_p) \Gamma_M(0; \mathbf{p}) G(\mathbf{p}, \omega_p) \frac{1}{2\kappa |\mathbf{p} - \mathbf{k}|}$$

In this case it makes a difference to choose

$$M_0 = \gamma_0 \begin{pmatrix} \sigma_3 & 0 \\ 0 & \sigma_3 \end{pmatrix} \quad \text{or} \quad M_H = i\gamma_1\gamma_2 \begin{pmatrix} \sigma_3 & 0 \\ 0 & -\sigma_3 \end{pmatrix}$$

which is a quantum anomaly, since it comes as a result of regularizing the many-body theory.

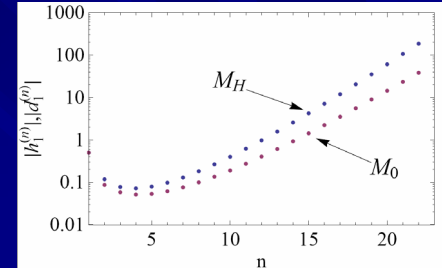
2D DIRAC SEMIMETALS

It turns out that the perturbative series diverges faster for M_H ,

$$\gamma_M = \frac{\mu}{Z_M} \frac{\partial Z_M}{\partial \mu} = -\lambda \tilde{d}'_1(\lambda) \quad , \quad \tilde{d}_1(\lambda) = \sum_{n=1}^{\infty} \tilde{d}_1^{(n)} \lambda^n$$

$$\lambda_c \approx 0.5448 \quad \text{for} \quad M_0 = \sigma_3 \otimes \mathbf{1}$$

$$\lambda_c \approx 0.508 \quad \text{for} \quad M_H = \sigma_3 \otimes \tau_3$$



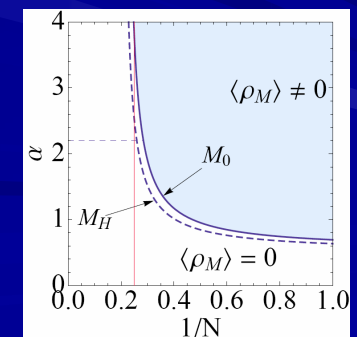
We have to make again the passage from the coupling λ to the nominal coupling $\alpha = e^2/4\pi v_F$

$$\lambda = \frac{\alpha}{1 + \frac{N\pi}{8}\alpha} \quad \Rightarrow \quad \alpha_c = \frac{\lambda_c}{1 - \frac{N\pi}{8}\lambda_c}$$

with the result that

$$\alpha_c \approx 3.78 \quad (N=4) \quad \text{for} \quad M_0 = \sigma_3 \otimes \mathbf{1}$$

$$\alpha_c \approx 2.51 \quad (N=4) \quad \text{for} \quad M_H = \sigma_3 \otimes \tau_3$$



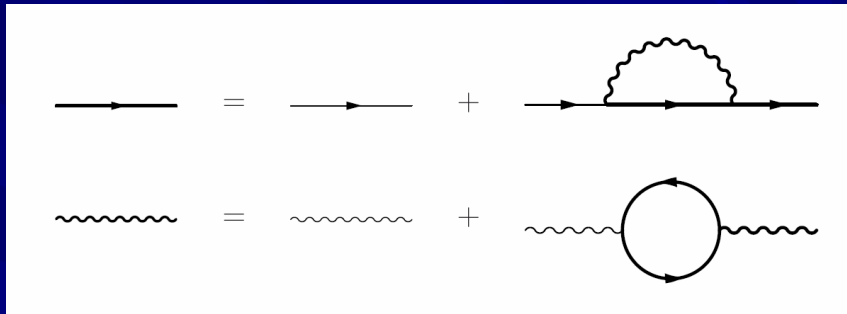
2D AND 3D DIRAC SEMIMETALS

The investigation of the strong-coupling system requires in general a nonperturbative approach

Here we propose the resolution of the Schwinger-Dyson equations (bare vertex approximation):

$$G^{-1}(\mathbf{k}, \omega) = \omega - v_F \gamma_0 \boldsymbol{\gamma} \cdot \mathbf{k} - \Sigma(\mathbf{k}, \omega)$$

$$D^{-1}(\mathbf{q}, \omega) = \frac{\mathbf{q}^2}{e^2} - \Pi(\mathbf{q}, \omega)$$



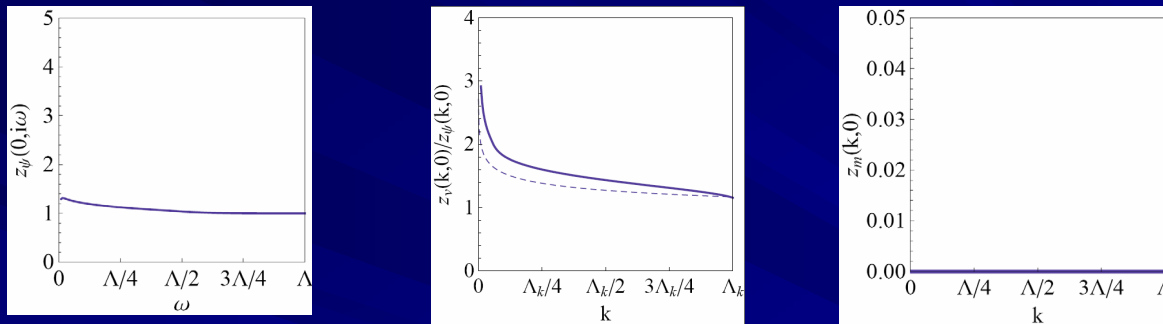
The self-consistent solution for the Dirac fermion propagator

$$G(\mathbf{k}, \omega) = \frac{1}{z_\psi(\mathbf{k}, \omega) \omega - z_v(\mathbf{k}, \omega) v_F \gamma_0 \boldsymbol{\gamma} \cdot \mathbf{k} + z_m(\mathbf{k}, \omega) \gamma_0}$$

encodes then the renormalization of the quasiparticle parameters.

2D DIRAC SEMIMETALS

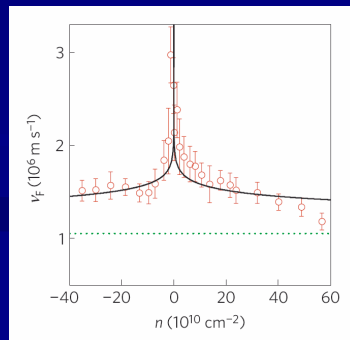
The self-consistent solution for the fermion propagator shows a renormalization of quasiparticle parameters in which $z_\psi(\mathbf{k},\omega)$ remains bounded while $z_v(\mathbf{k},\omega)$ diverges in the low-energy limit



$$\alpha = 2.2$$

J.G., PRB **92**, 125115 (2015)

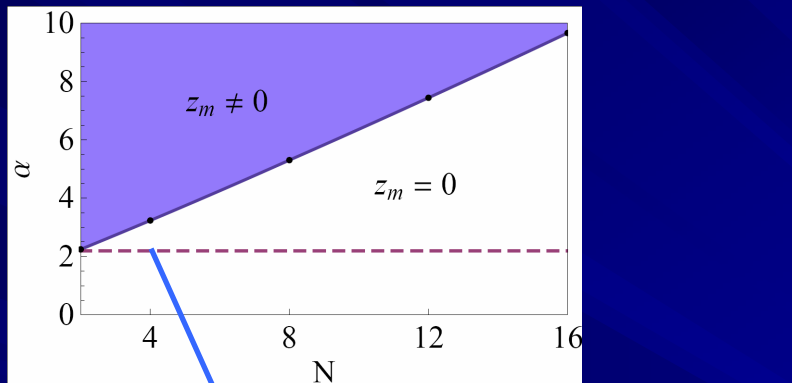
This increase of the Fermi velocity is in agreement with the experimental results in graphene



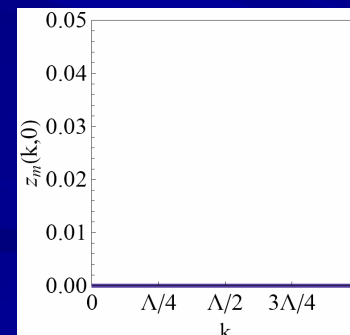
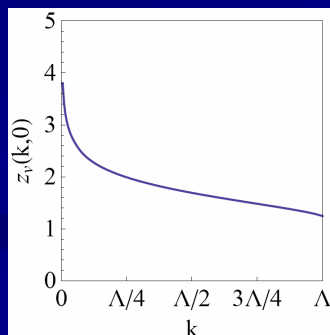
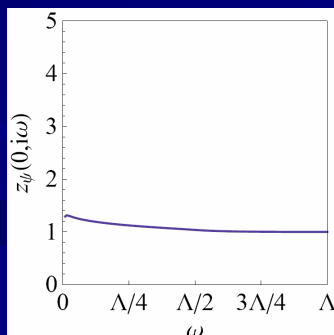
D. C. Elias *et al.*, Nature
Phys. **7**, 701 (2011)

2D DIRAC SEMIMETALS

But in general we may expect two different phases in 2D Dirac semimetals, depending on whether a mass is dynamically generated for the Dirac fermions



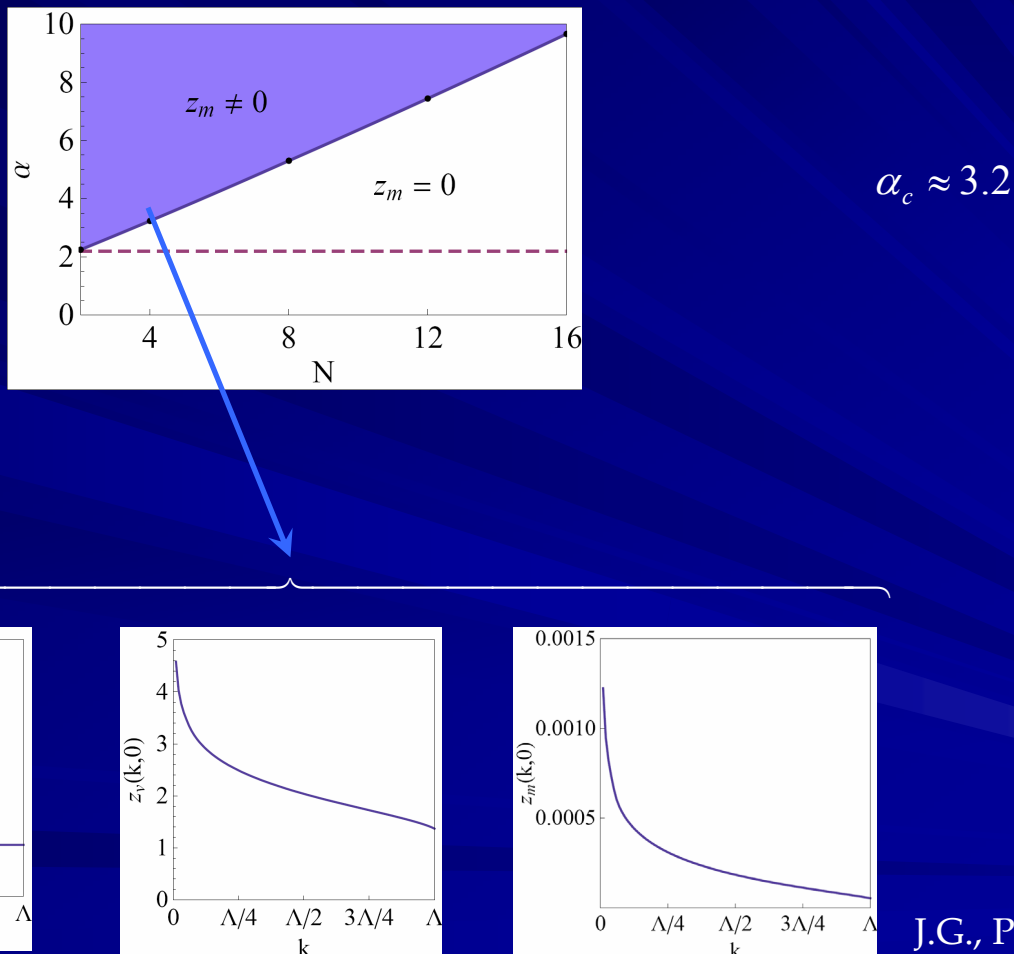
$$\alpha = 2.2$$



J.G., PRB **92**, 125115 (2015)

2D DIRAC SEMIMETALS

But in general we may expect two different phases in 2D Dirac semimetals, depending on whether a mass is dynamically generated for the Dirac fermions



J.G., PRB **92**, 125115 (2015)

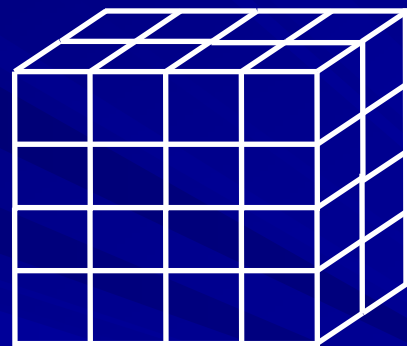
2D DIRAC SEMIMETALS

The fact that the dynamical breakdown of parity and chiral symmetry does not take place at the same λ_c can be considered as an anomaly (a consequence of the regularization at $D = 2 - \varepsilon$) since $\sigma_3 \otimes \mathbf{1}$ and $\sigma_3 \otimes \tau_3$ should have the same effect in the ladder approximation

In order to check this anomaly, we can look at the other regularization commonly used in gauge invariant theories, given by the lattice formulation of the Dirac fermions

$$S = \int dt d^2r \bar{\Psi}(\mathbf{r}) i(\gamma_0 \partial_t - \boldsymbol{\gamma} \cdot \boldsymbol{\partial}) \Psi(\mathbf{r})$$

$$\Rightarrow \sum_{\mathbf{n}, \mu=0,1,2} \bar{\Psi}(\mathbf{n}) \gamma_\mu (\Psi(\mathbf{n} + \mathbf{e}_\mu) - \Psi(\mathbf{n} - \mathbf{e}_\mu))$$



We will use the formulation of staggered fermions, defined by the change of variables

$$\bar{\Psi}(\mathbf{n}) = \bar{\chi}(\mathbf{n}) \gamma_2^{n_2} \gamma_1^{n_1} \gamma_0^{n_0} , \quad \Psi(\mathbf{n}) = \gamma_0^{n_0} \gamma_1^{n_1} \gamma_2^{n_2} \chi(\mathbf{n})$$

and which have the advantage of rendering the action diagonal

$$S = \sum_{\mathbf{n}, \mu=0,1,2} \eta_\mu(\mathbf{n}) \bar{\chi}_\sigma(\mathbf{n}) (\chi_\sigma(\mathbf{n} + \mathbf{e}_\mu) - \chi_\sigma(\mathbf{n} - \mathbf{e}_\mu))$$

2D DIRAC SEMIMETALS

The interaction with the scalar potential A_0 can be introduced in the usual fashion

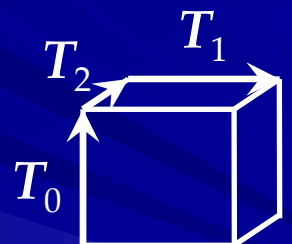
$$S = \sum_{\mathbf{n}, \mu=0,1,2} \eta_\mu(\mathbf{n}) \left(\bar{\chi}(\mathbf{n}) U(\mathbf{n} + \mathbf{e}_\mu) \chi(\mathbf{n} + \mathbf{e}_\mu) - \bar{\chi}(\mathbf{n}) U^+(\mathbf{n}) \chi(\mathbf{n} - \mathbf{e}_\mu) \right) + \frac{\beta}{2} \sum_{\mathbf{n}} \left(\sum_{i=1,2,3} (A_0(\mathbf{n}) - A_0(\mathbf{n} + \mathbf{e}_i))^2 \right) \quad \beta \equiv \frac{v_F}{e^2}$$

The staggered fermions have also the advantage of preserving a residual chiral symmetry

$$\chi(\mathbf{n}) \rightarrow \exp\left((-1)^{n_0+n_1+n_2} i\theta\right) \chi(\mathbf{n}) \quad , \quad \bar{\chi}(\mathbf{n}) \rightarrow \exp\left((-1)^{n_0+n_1+n_2} i\theta\right) \bar{\chi}(\mathbf{n})$$

In this formulation, the Dirac fermion components are spread over each unit cell of the lattice, which explains that the mass matrices M_0 and M_H are realized in different ways:

$$\begin{aligned} M_0 &= \gamma_0 \quad \Rightarrow \quad S_0 = m_0 \sum_{\mathbf{n}} \bar{\chi}(\mathbf{n}) \chi(\mathbf{n}) \\ M_H &= i \gamma_1 \gamma_2 \quad \Rightarrow \quad S_H = m_H \sum_{\mathbf{n}} \bar{\chi}(\mathbf{n}) i \sum_{ijk} \eta_0 \eta_1 \eta_2 T_i T_j T_k \chi(\mathbf{n}) \end{aligned}$$



One is led therefore to compute the susceptibilities

$$\chi_0 = \left. \frac{\partial \langle \bar{\chi}(\mathbf{n}) \chi(\mathbf{n}) \rangle}{\partial m_0} \right|_{m_0=0} \quad \chi_H = \left. \frac{\partial \langle \bar{\chi}(\mathbf{n}) i \sum_{ijk} \eta_0 \eta_1 \eta_2 T_i T_j T_k \chi(\mathbf{n}) \rangle}{\partial m_H} \right|_{m_H=0}$$

2D DIRAC SEMIMETALS

In practice, we perform a Monte Carlo simulation of the susceptibility

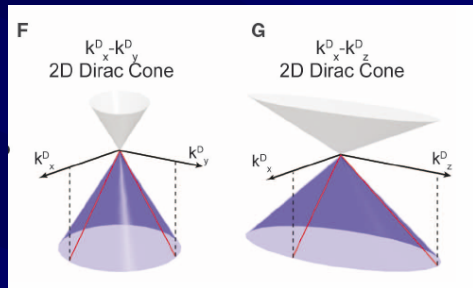
$$\chi_M = \frac{\partial \langle \bar{\chi}(\mathbf{n}) M \chi(\mathbf{n}) \rangle}{\partial m_M} \Bigg|_{m_M=0} = \frac{\partial}{\partial m_M} Z^{-1} \int \prod_{\mathbf{n}} d\chi(\mathbf{n}) d\bar{\chi}(\mathbf{n}) dA_0(\mathbf{n}) (\bar{\chi}(\mathbf{n}) M \chi(\mathbf{n})) \exp(-S - S_M) \Bigg|_{m_M=0}$$

Computing with dynamical fermions, the results for the susceptibilities have in general inflection points, in agreement with what is expected for a Kosterlitz-Thouless transition:

In the case of chiral symmetry breaking, $\beta_c < 0.056 \Rightarrow e^2/4\pi v_F > 1.4$. But the bad news are that the finite size scaling of the critical coupling should be given by $\beta_c(L) - \beta_c \sim 1/\log^2(L)$.

3D DIRAC SEMIMETALS

3D semimetals are materials hosting Dirac cones with linear dispersion in all three dimensions:



Z. K. Liu *et al.*, Science **343**, 864 (2014)

Na_3Bi

M. Neupane *et al.*, Nature Commun. **5**, 3786 (2014)

Cd_3As_2

S. Borisenko *et al.*, Phys. Rev. Lett. **113**, 027603 (2014)

Cd_3As_2

The low-energy electronic states in Na_3Bi and Cd_3As_2 can be naturally arranged into four-component spinors around each of two Dirac points, with Dirac matrices in the chiral representation

$$\gamma_0 \gamma_i = \eta_i \begin{pmatrix} \sigma_i & 0 \\ 0 & -\sigma_i \end{pmatrix} \quad , \quad \gamma_0 = \begin{pmatrix} 0 & -\mathbf{1} \\ -\mathbf{1} & 0 \end{pmatrix}$$

3D DIRAC SEMIMETALS

We focus again on the effects of the long-range Coulomb interaction in 3D

$$H = \sum_{i=1}^N \int d^3x \Psi_i^+(\mathbf{x}) i v_F \gamma_0 \boldsymbol{\gamma} \cdot \boldsymbol{\partial} \Psi_i^-(\mathbf{x}) + e_0 \int d^3x \sum_{i=1}^N \Psi_i^+(\mathbf{x}) \Psi_i^-(\mathbf{x}) A_0(\mathbf{x})$$

The important difference is that now the polarization depends on the high-energy cutoff



$$\Pi_0(\mathbf{q}, \omega) = \frac{N}{12\pi^2 v_F} \mathbf{q}^2 \log\left(\frac{\Lambda^2}{\mathbf{q}^2 - \omega^2 / v_F^2}\right)$$

The Coulomb propagator shows then an apparent dependence on Λ

$$D(\mathbf{q}, \omega) = -\frac{e_0^2}{\mathbf{q}^2 + \frac{Ne_0^2}{12\pi^2 v_F} \mathbf{q}^2 \log\left(\frac{\Lambda^2}{\mathbf{q}^2 - \omega^2 / v_F^2}\right)}$$

which must be compensated by the dependence of the bare coupling $e_0(\Lambda)$

$$\frac{1}{e^2} = \frac{1}{e_0^2(\Lambda)} + \frac{N}{12\pi^2 v_F} \log(\Lambda^2) \quad \Rightarrow \quad e_0^2(\Lambda) = \frac{e^2}{1 - \frac{Ne^2}{12\pi^2 v_F} \log(\Lambda^2)}$$

3D DIRAC SEMIMETALS

The theory can be solved in the large- N limit, showing as a main effect the strong attenuation of electron quasiparticles:

$$\Sigma(\mathbf{k}, \omega) = \sum_{n=1}^{\infty} \text{Diagram } n$$

$$\frac{1}{G} = Z_\omega (\omega - Z_\nu v_F \gamma_0 \boldsymbol{\gamma} \cdot \mathbf{k}) - \Sigma$$

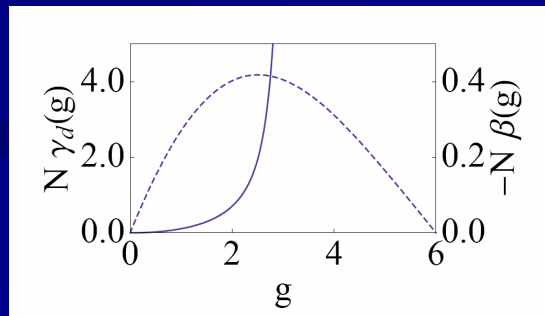
The electron quasiparticles get an anomalous dimension, while v_F also scales at low energies

$$G(s\mathbf{k}, s\omega) = s^{-1+\gamma} G(\mathbf{k}, \omega)$$

with

$$\gamma(g) = \frac{\mu}{Z_\omega} \frac{\partial Z_\omega}{\partial \mu} \quad \beta(g) = \frac{\mu}{v_F} \frac{\partial v_F}{\partial \mu} \quad , \quad g \equiv \frac{Ne^2}{2\pi^2 v_F}$$

At large N , we find that $\gamma(g)$ diverges at a critical coupling $g_c = 3$



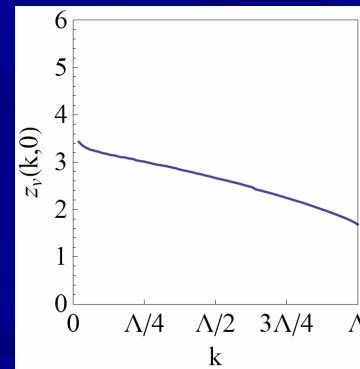
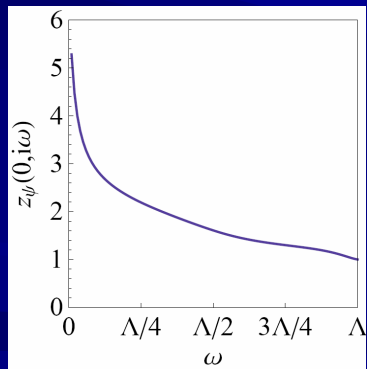
3D DIRAC SEMIMETALS

3D Dirac semimetals have in general a behavior quite different to that of their 2D analogues

A self-consistent resolution of the Schwinger-Dyson equations is again possible with

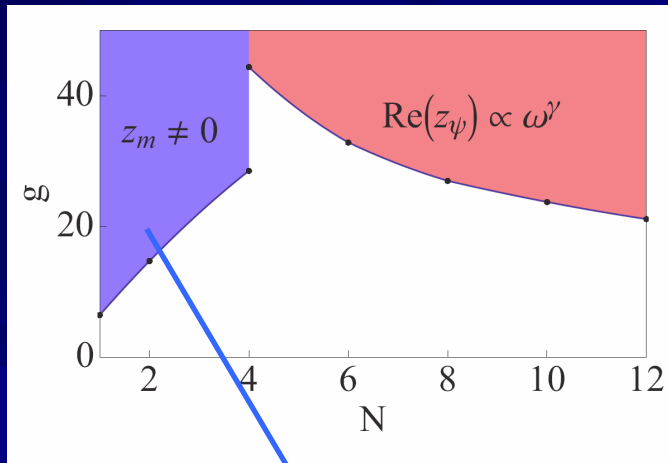
$$G(\mathbf{k}, \omega) = \frac{1}{z_\psi(\mathbf{k}, \omega) \omega - z_v(\mathbf{k}, \omega) v_F \gamma_0 \gamma \cdot \mathbf{k} + z_m(\mathbf{k}, \omega) \gamma_0}$$

But now the most significant feature is the attenuation of electron quasiparticles at low energies

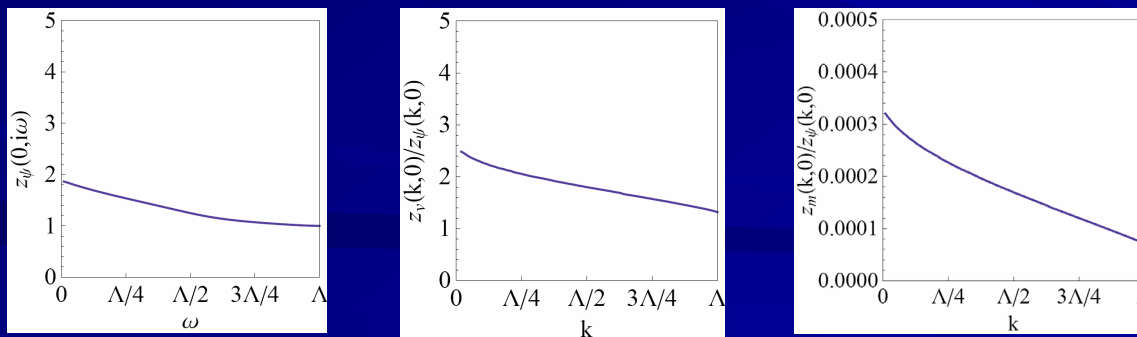


3D DIRAC SEMIMETALS

3D Dirac semimetals have a richer phase diagram depending on the number N of Dirac fermions

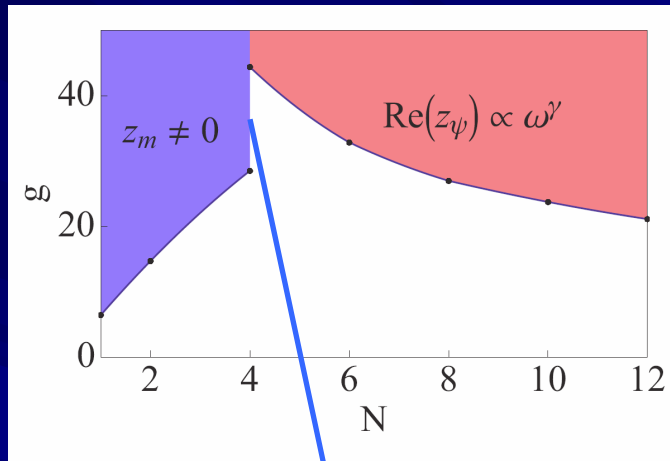


$$g \equiv \frac{Ne^2}{4\pi v_F}$$

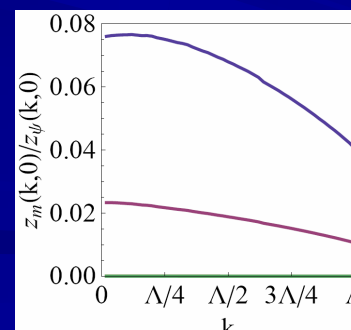
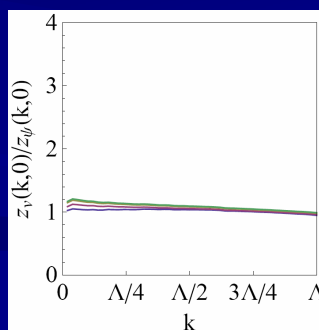
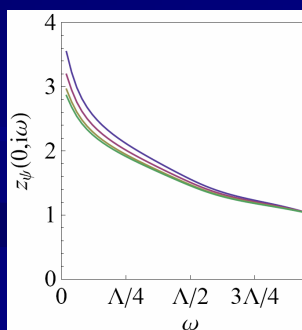


3D DIRAC SEMIMETALS

3D Dirac semimetals have a richer phase diagram depending on the number N of Dirac fermions

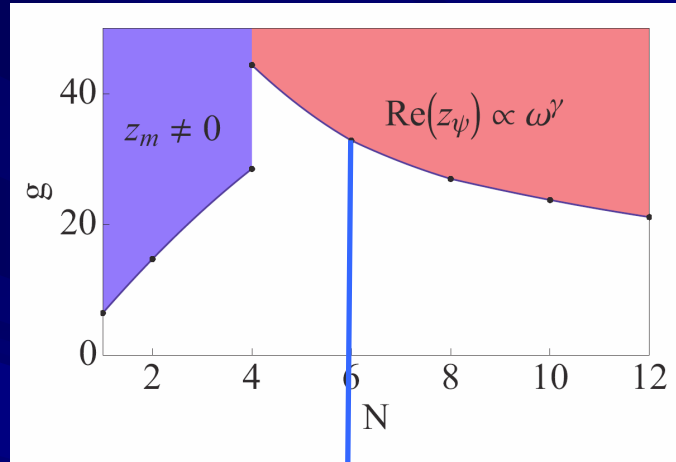


$$g \equiv \frac{Ne^2}{4\pi v_F}$$

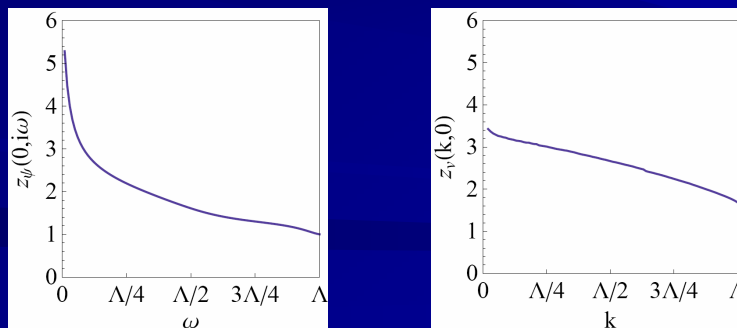


3D DIRAC SEMIMETALS

3D Dirac semimetals have a richer phase diagram depending on the number N of Dirac fermions

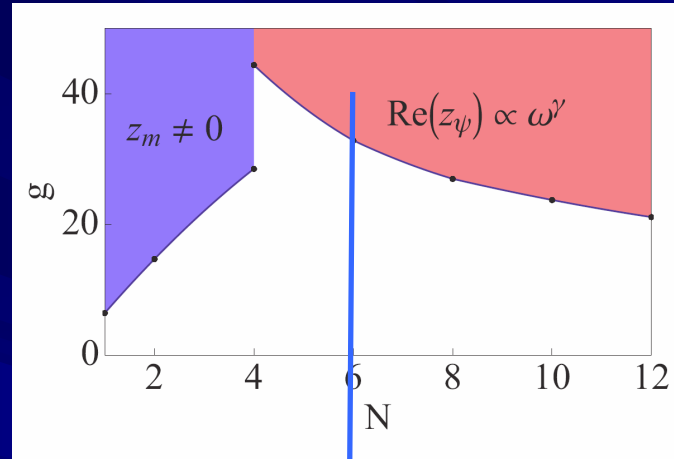


$$g \equiv \frac{Ne^2}{4\pi v_F}$$

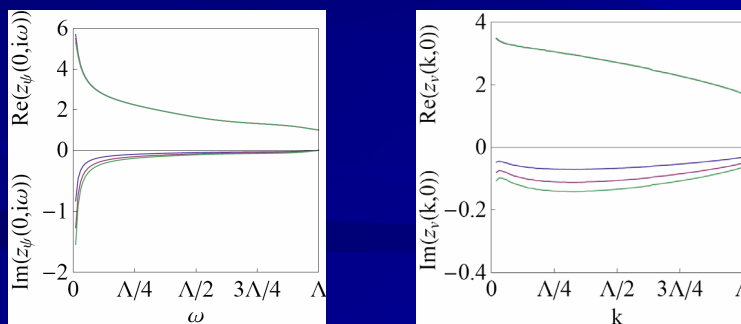


3D DIRAC SEMIMETALS

3D Dirac semimetals have a richer phase diagram depending on the number N of Dirac fermions



$$g \equiv \frac{Ne^2}{4\pi v_F}$$



DIRAC SEMIMETALS

In conclusion,

- Dirac semimetals are electron systems with important many-body effects, which have to be considered appropriately to account for the experimental observations
- In the case of graphene, the maximum coupling reached in suspended samples should be well below the critical point for exciton condensation, but closer to the transition to the phase with dynamical generation of Haldane mass
- On the other hand, 3D Dirac semimetals have a richer phase diagram depending on the number N of Dirac fermions, with a strong-coupling instability leading to dynamical mass generation up to $N = 4$ and a line of critical points for larger values of N characterized by the vanishing of the electron quasiparticle weight in the low-energy limit. Such a critical behavior signals the transition to a strongly correlated liquid, characterized by noninteger scaling dimensions that are the signature of non-Fermi liquid behavior